Electrodeposition of Si Film from Water-Soluble KF-KCl Molten Salt and Feasibility of $SiCl_4$ as a Si Source

Kouji Yasuda[a,b], Kazumi Saeki[a], Kazuma Maeda[a],
Toshiyuki Nohira[c], Rika Hagiwara[a] and Takayuki Homma[d]

[a] Graduate School of Energy Science, Kyoto University, Kyoto 606-8501, Japan
[b] Environment, Safety and Health Organization, Kyoto University, Kyoto 606-8501, Japan
[c] Institute of Advanced Energy, Kyoto University, Uji 611-0011, Japan.
[d] Faculty of Science and Engineering, Waseda University, Tokyo 169-8555, Japan.

Toward an establishment of a new production method of solar cell substrates, electrodeposition of Si was investigated in molten KF–KCl (eutectic composition, 45:55 mol%) after the introduction of $SiCl_4$. Gaseous $SiCl_4$ was directly introduced into the molten salt at 1023 K by a vapor transport method using Ar carrier gas. The dissolution ratio of $SiCl_4$ exceeded 80% even with the use of a simple tube for the bubbling. Galvanostatic electrolysis was conducted at 923 K on a Ag substrate at 155 mA cm^{-2} for 20 min in molten KF–KCl after the dissolution of 2.30 mol% $SiCl_4$. Although compact Si layer was formed, the smoothness was lower compared to that obtained from the melt after the addition of K_2SiF_6. The anionic molar fraction is probably one of the factors affecting the morphology of deposit.

Introduction

The current production of Si substrates of photovoltaic cells is composed of multiple processes including a slicing-step of high-purity Si ingots prepared in the Siemens process. This method has several drawbacks in terms of energy efficiency and yield because of the low productivity of the Siemens process and the considerable kerf loss in the slicing-step. Therefore, the development of an alternative and efficient process for manufacturing crystalline Si substrates is important and would make a great breakthrough for photovoltaic industry.

Direct formation of Si films has been investigated as one of the alternative methods for producing polycrystalline Si solar cells. The electrodeposition of crystalline Si has been reported in high-temperature molten salts since the 1970's (1–9). The use of fluoride-based molten salts, such as LiF–KF and LiF–NaF–KF, is effective for obtaining compact and smooth Si films. However, a major problem in the previous investigations employing fluoride-based molten salts is the removal of the salt adhered to the deposited Si, because the solubilities of LiF and NaF in water are very low. Another inherent problem is the lack of availability of high-purity and low-cost Si sources. Conventionally, either K_2SiF_6 or anodic dissolution of a Si rod has been utilized for supplying Si ions. However, preparation of K_2SiF_6 and Si rods of solar grade purity at low costs is difficult.

With the aim of developing a new production method of polycrystalline Si films for solar cells, our group has proposed and investigated a new electrodeposition process for

Si using KF–KCl as a molten salt electrolyte and high-purity gaseous $SiCl_4$ as a Si source (Fig. 1) (10–12). In this process, gaseous $SiCl_4$ is introduced into the molten salt to produce Si(IV) complex ions. Si films are then electrodeposited onto a cathode of an appropriate material, and Cl_2 gas is evolved at a carbon anode. The salt adhered on the Si deposit can be easily removed by washing with water.

$SiCl_4$ dissolution:	$SiCl_4\,(g) + 6\,F^- \rightarrow SiF_6^{2-} + 4\,Cl^-$	[1]
Cathodic reaction:	$SiF_6^{2-} + 4\,e^- \rightarrow Si\,(s) + 6\,F^-$	[2]
Anodic reaction:	$4\,Cl^- \rightarrow 2\,Cl_2\,(g) + 4\,e^-$	[3]
Total reaction:	$SiCl_4\,(g) \rightarrow Si\,(s) + 2\,Cl_2\,(g)$	[4]

In this process, Si electrodeposition is achieved without introducing impurities or changing the composition of the molten salt. Moreover, when the Cl_2 gas by-product is recovered for the chlorination of Si to produce $SiCl_4$, a circulation cycle generating no by-product is realized. One of the advantages of our proposed process is the high solubility of the solidified KF–KCl salt to water (KF; 101.6 g 100 g-H_2O^{-1}, LiF; 0.13 g 100 g-H_2O^{-1}, NaF; 0.15 g 100 g-H_2O^{-1}, MgF_2; 0.13 g 100 g-H_2O^{-1}, CaF_2; 0.0016 g 100 g-H_2O^{-1} (13)). This molten salt must be a unique solution to achieve both high solubility to water and the use of fluoride salt which is essential to obtain compact and smooth Si films. In our previous studies (10–12), the electrodeposition of Si from Si(IV) complex ions on a Ag electrode was investigated in a molten KF–KCl–K_2SiF_6 system at 923 K as the first research before introducing $SiCl_4$ gas to the molten salt. The Si films electrodeposited from KF–KCl molten salt containing 0.5–5.0 mol% K_2SiF_6 had adherent, compact, and smooth characteristics. Further, the residual salt on the deposited Si was confirmed to be easily removed only by washing with water.

In the present study, we investigated the feasibility of the use of $SiCl_4$ gas as a Si source. Gaseous $SiCl_4$ was introduced to molten KF–KCl by a vapor transport method using Ar as a carrier gas. The electrodeposits were obtained by galvanostatic electrolysis from the melt. The deposited Si was analyzed by cross-sectional scanning electron microscopy (SEM) and energy-dispersive X-ray spectroscopy (EDX).

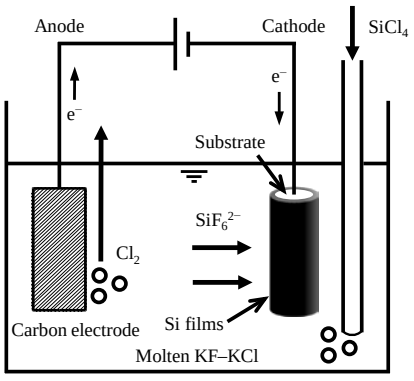

Figure 1. A schematic illustration for the principle of electroplating process of Si in KF–KCl molten salt (10,11).

Experimental

The experimental setup is schematically illustrated in Fig. 2. Reagent-grade KF (Wako Pure Chemical Co. Ltd., >99.0%) and KCl (Wako Pure Chemical Co. Ltd., >99.5%) were

mixed to the eutectic composition (45 mol%KF + 55 mol%KCl, melting point = 878 K (14)) and loaded in a graphite crucible (Toyo Tanso Co. Ltd., o.d. 90 mm, i.d.: 80 mm, height: 120 mm). The mixture in the crucible was first dried under vacuum at 453 K for 72 h to remove residual moisture. The crucible was placed at the bottom of a quartz vessel in an air-tight Kanthal container with a stainless steel lid. The salt was further dried under vacuum at 673 K for 24 h. The experiments were conducted in a dry Ar atmosphere at 923 K or 1023 K. Liquid $SiCl_4$ (Aldrich, 99.998%) held in a Duran® bottle (100 mL) was maintained at 293 K in a water bath using a thermostat (As-one, Cool Circulator CH-202). Pyrex® pipes (o.d.: 6 mm, i.d.: 4 mm) connected to perfluoro alkoxy alkane (PFA) tubes (o.d.: 6.35 mm, i.d.: 4.35 mm) were attached to the screw cap (As-one, pipe diam.: 6–8 mm) of the bottle. The mixed Ar–$SiCl_4$ gas was prepared by bubbling 20 mL min^{-1} of Ar gas (Kyoto Teisan, Inc., >99.998%) into liquid $SiCl_4$ using the Pyrex® pipe. The mixed gas was bubbled into 200 g of eutectic molten KF–KCl at 1023 K with a graphite pipe (Toyo Tanso Co., Ltd., ISO-68TS, o.d.: 12 mm, i.d.: 5 mm, length: 470 mm). After bubbling the mixed gas for the predetermined period, the lower end of the pipe was removed from the melt and the flow gas was switched to pure Ar. Then, the temperature of the melt was lowered to 923 K, and electrochemical measurements were carried out. The working electrodes were Ag wire (Nilaco Corp., diam.: 0.1 mm, 99.98%) and Ag flag electrodes (Nilaco Corp., thickness: 0.1 mm, 99.98%) (11). A glass-like carbon rod (Tokai Carbon Co., Ltd., diam.: 5.0 mm) was used as the counter electrode. A Pt wire (Tanaka Kikinzoku Kogyo, >99.95%, diam.: 1.0 mm) was employed as the quasi-reference electrode. The potential of the reference electrode was calibrated with reference to a dynamic K^+/K potential, which was prepared by the electrodeposition of K metal on a Ag wire. The electrolyzed samples were washed in hot distilled water at 333 K for 24 h to remove the adhered salt on the deposits and dried under vacuum for 12 h. The samples were analyzed by SEM (Keyence Corp., VE-8800) and EDX (AMETEK Co. Ltd., EDAX Genesis APEX2). For the cross-sectional SEM observations, the samples were embedded in acrylic resin and polished with emery paper and buffing compound.

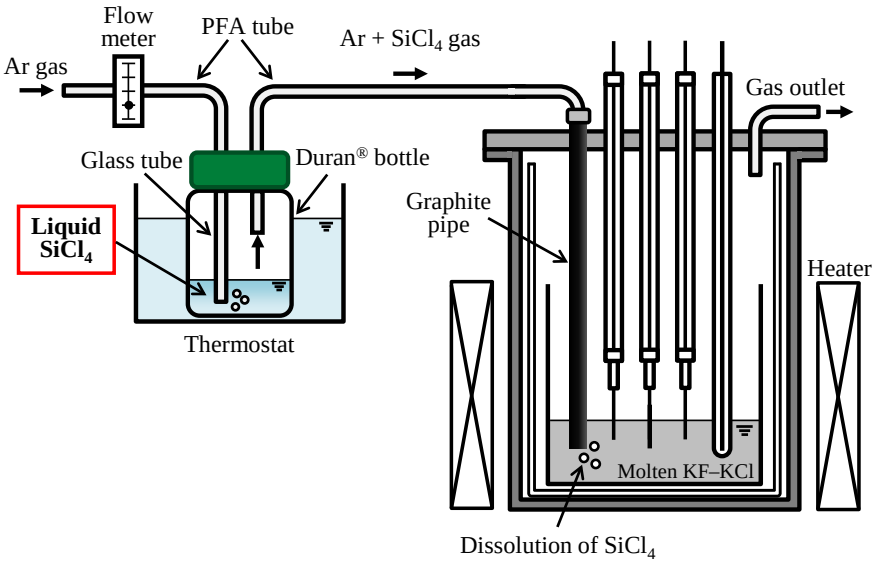

Figure 2. A schematic drawing of the experimental apparatus for the introduction of $SiCl_4$ by a vapor transport method.

Thermodynamic Calculation

Figure 3 shows the Gibbs energies for the reactions of the chlorides with fluorine gas to form the fluorides and chlorine gas (15).

$$\frac{2}{x}\mathrm{SiCl}_x\ (l, g) + \mathrm{F}_2\ (g) = \frac{2}{x}\mathrm{SiF}_x\ (l, g) + \mathrm{Cl}_2\ (g) \quad (x = 1, 2, 3, 4) \qquad [5]$$

$$2\ \mathrm{KCl}\ (s, l) + \mathrm{F}_2\ (g) = 2\ \mathrm{KF}(s, l) + \mathrm{Cl}_2\ (g) \qquad [6]$$

As indicated in the figure, the Gibbs energy of reaction for the formation of SiF_4 and Cl_2 from $SiCl_4$ and F_2 is much more negative compared to the case of KF and KCl. Thus, the converstion of $SiCl_4$ to SiF_4 in the reaction with KF is thermodynamically favorable.

$$\frac{1}{2}\mathrm{SiCl}_4\ (g) + 2\ \mathrm{KF}(l) = \frac{1}{2}\mathrm{SiF}_4\ (g) + 2\ \mathrm{KCl}\ (l) \qquad [7]$$

$$\Delta G_\mathrm{r}^\circ = -\ 221.17\ \mathrm{kJ} \quad \text{at } 923\ \mathrm{K}\ \ (15)$$

In the same manner, the conversion of Si chlorides with lower oxidation states to the corresponding fluorides is expected to proceed. Considering the thermodynamic calculations, the $SiCl_4$ gas introduced into KF–KCl melt is expected to dissolve to produce SiF_6^{2-} complex ions which are highly stable in molten salts.

$$\mathrm{SiCl}_4\ (g) + 6\ \mathrm{F}^- \rightarrow \mathrm{SiF}_6^{2-} + 4\ \mathrm{Cl}^- \qquad [8]$$

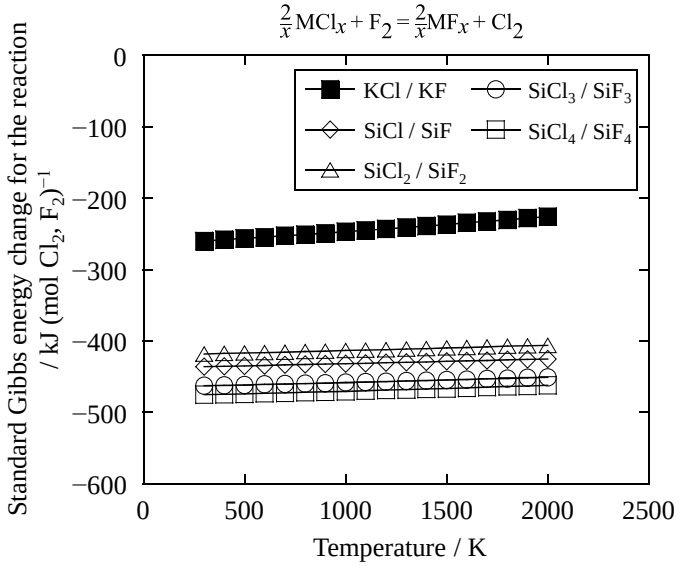

Figure 3. Standard Gibbs energy changes for the reactions of chlorides and F_2 gas to form fluorides and Cl_2 gas (15).

Results and discussion

Vapor transport of $SiCl_4$

The supply of $SiCl_4$ was conducted via a vapor transport method utilizing Ar carrier gas and the apparatus shown in Fig. 2. The transport rate was controlled by the flow rate of Ar gas and the partial pressure of $SiCl_4$ in the mixed Ar–$SiCl_4$ gas using a gas flowmeter and a thermostat, respectively. The vapor pressure of $SiCl_4$, P_{SiCl_4}, changes with the temperature, T, according to the following equations (16).

$$P_{SiCl_4} = 10^{\left(4.0977-\frac{1200}{T-37}\right)} \qquad (275 < T < 330\ \mathrm{K}) \qquad [9]$$

In the present experiment system, the total gas pressure is 1 atm,

$$P_{Ar} + P_{SiCl_4} = 1\ \mathrm{atm} \qquad [10]$$

where P_{Ar} is the partial pressure of Ar. Thus, the flow volume rate of $SiCl_4$, f_{SiCl_4}, is expressed as a function of the rate of Ar, f_{Ar}, at 298 K.

$$f_{SiCl_4} = f_{Ar} \cdot \frac{P_{SiCl_4}}{P_{Ar}} = f_{Ar} \cdot \frac{P_{SiCl_4}}{1-P_{SiCl_4}} \qquad [11]$$

Therefore, the transport rate of $SiCl_4$, v_{SiCl_4}, is

$$v_{SiCl_4} = \frac{P_0}{RT} \cdot f_{SiCl_4} = \frac{P_0}{RT} \cdot \frac{P_{SiCl_4}}{1-P_{SiCl_4}} \cdot f_{Ar} \qquad [12]$$

where R is the gas constant and P_0 is the ambient atmospheric pressure (1.013×10^5 Pa).

The above relationships are valid only when the evaporation is fast enough to reach the equilibrium. To confirm this, the folowing experiments were conducted. As the experimental conditions, bath temperature and gas flow rate were set at T = 293 K (P_{SiCl_4} = 0.257 atm) and f_{Ar} = 20 mL min^{-1}. First, 20 mL min^{-1} of Ar gas was flown into liquid $SiCl_4$ at 293 K for 50 min, and the weight change was measured. The transport rate of $SiCl_4$, v_{SiCl_4}, was calculated according to Eqs. 13 and 14.

$$W_{SiCl_4,\,trans} = W_{SiCl_4,\,bef} - W_{SiCl_4,\,aft} \qquad [13]$$

$$v_{SiCl_4} = \frac{W_{SiCl_4,\,trans}}{M_{SiCl_4} \cdot t} \qquad [14]$$

Here, $W_{SiCl_4,\,bef}$ and $W_{SiCl_4,\,aft}$ represent the total weight of liquid $SiCl_4$ and Duran® bottle before and after the Ag gas flow, respectively. The value of $W_{SiCl_4,\,trans}$ means the weight of transported $SiCl_4$ in the duration time. As shown in Table 1 (Exp. #4-1), the value of v_{SiCl_4} was calculated to be 2.86×10^{-4} mol min^{-1} from $W_{SiCl_4,\,trans}$ = 2.43 g and Eq. 14. Meanwhile, the theoretical value of v_{SiCl_4} from Eq. 12 was 2.83×10^{-4} mol min^{-1}. The agreement confirms that the precise control of $SiCl_4$ supply is possible in the present vapor transport method.

Table 1 Transport rate of $SiCl_4$ by vapor transport method.

Exp. #	Temperature of $SiCl_4$ T / K	Vapor pressure of $SiCl_4$ [a] P_{SiCl_4} / atm	Ar flow rate at 298 K f_{Ar} / mL min^{-1}	Reaction time t / min	Weight of $SiCl_4$ / g			Transport rate v_{SiCl_4} / mol min^{-1}
					Before reaction $W_{SiCl_4, bef}$	After reaction $W_{SiCl_4, aft}$	Transported [b] $W_{SiCl_4, trans}$	
# 4-1	293	0.257	20	50	250.55	248.12	02.43	2.86×10^{-4} [c]
Calculated	293	0.257	20	50	—	—	—	2.83×10^{-4} [d]
# 4-2	293	0.257	20	310	256.00	241.10	14.90	2.83×10^{-4} [c]
Calculated	293	0.257	20	310	—	—	—	2.83×10^{-4} [d]

a: $P_{SiCl_4} = 10^{\left(4.0977-\frac{1200}{T-37}\right)}$ b: $W_{SiCl_4, trans} = W_{SiCl_4, bef} - W_{SiCl_4, aft}$ c: $v_{SiCl_4} = \frac{W_{SiCl_4, trans}}{M_{SiCl_4} \cdot t}$ d: $v_{SiCl_4} = \frac{P_0}{RT} \cdot f_{SiCl_4} \cdot 10^{-6} = \frac{P_0}{RT} \cdot \frac{P_{SiCl_4}}{1 - P_{SiCl_4}} \cdot f_{Ar} \cdot 10^{-6}$

Injection of $SiCl_4$ into molten KF–KCl

In our previous study, the adequate condition for the electrodeposition of adherent, compact, and smooth Si layers in molten KF–KCl–K_2SiF_6 at 923 K were found to be intermediate K_2SiF_6 concentrations (2.0–3.5 mol%) and current densities (50–200 mA cm^{-2}) (12). Thus, 2.86 mol% of $SiCl_4$ with respect to the eutectic KF–KCl salt was injected by bubbling the mixed Ar–$SiCl_4$ gas with the vapor transport method. As the result, 14.90 g of gaseous $SiCl_4$ was transported from the liquid $SiCl_4$ to 200 g of KF–KCl melt at 1023 K. As shown in Table 1 (Exp. #4-2), both of the experimental and theoretical transport rates coincide with the value of 2.83×10^{-4} mol min^{-1}.

After the injection of $SiCl_4$, the bath temperature was lowered from 1023 K to 923 K, and the melt was investigated by cyclic voltammetry. The solid line in Fig. 4 shows the voltammogram obtained with a Ag flag electrode. In the potential sweep to negative direction, a cathodic current peak is observed at 0.57 V vs. K^+/K which is almost the same potential with Si deposition (11). Additionally, a small cathodic current shoulder is observed around 0.8 V, which is likely due to the reduction of impurities. The voltammogram is compared with that previously obtaied in the melt after the addition of 2.0 mol% K_2SiF_6, which is indicicated with the broken curve in Fig. 4. The peak current densities corresponding to Si deposition are –1.742 A cm^{-2} and –1.521 A cm^{-2} in the solid curve ($SiCl_4$) and the broken curve (K_2SiF_6), respectively. Since the peak current density is proportional to the Si ion concentration (11), the concentration of SiF_6^{2-} ions is estimated as 2.30 mol%. Thus, a melt with optimum Si ion concentration (2.0–3.5 mol%) for the compact electrodeposition was successfully prepared.

The dissolution efficiency of $SiCl_4$ was calculated to be 80% from the supplied amount (2.86 mol%) and the dissolved amount (2.30 mol%). In contrast, in the molten LiCl–KCl system at 723 K, the supplied $SiCl_4$ scarecely dissolved into the melt but evaporate into the gas phase (17). It should be especially noted that the high efficiency was achieved in this study even by bubbling with a simple pipe with an inner diameter of 5 mm. The contacting and reacting time between $SiCl_4$ gas and KF–KCl molten salt should have been very short in the present experimental system.

The high dissolution rate and soubility of $SiCl_4$ to the floride melt showed a high feasibility for the use of $SiCl_4$ and KF–KCl molten salt as a Si source and an electrolyte

for Si electrodepositon. The high reactivity is explained by the large driving force of reaction between $SiCl_4$ and KF, as seen in the thermodynamic calculation in Fig. 3 and Eq. 7. The dissolution efficiency will be easily and largely improved when finer bubbles are introduced by using a fine gas bubbler.

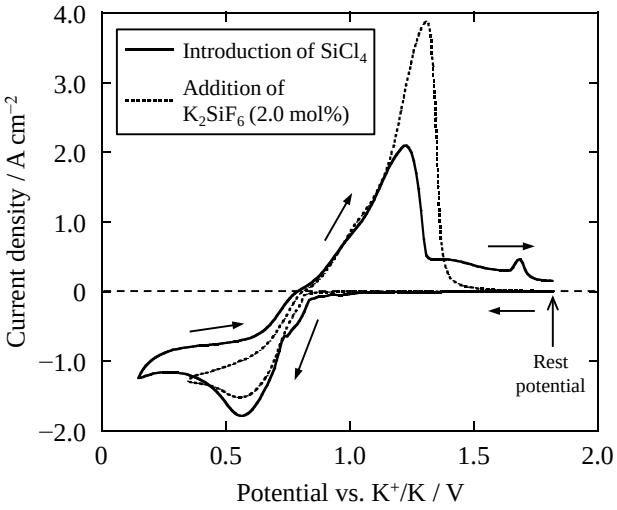

Figure 4. Cyclic voltammograms for a Ag flag electrode in molten KF–KCl–K_2SiF_6 (2.0 mol%) at 923 K and molten KF–KCl at 923 K after the introduction of $SiCl_4$. Scan rate: 0.50 V s^{-1}.

Electrodeposition of Si

Since the existence of some impurities in the melt was suggested by the voltammetry, pre-electrolysis was carried out to remove them. After the electrolysis at 0.95 V vs. K^+/K for 88 min, a black deposit was obtained on a Ag wire electrode. The deposit was found to be mainly consisted of iron metal by EDX. A small leakage of the gas supply system would lead to the reaction of $SiCl_4$ and moisture forming SiO_2 and hydrogen chloride. A stainless steel connector between the PFA tube and the graphite pipe was probably corroded by the hydrogen chloride gas and the iron chlorides were introduced into the molten salt.

After the pre-electrolysis, the electrodeposition of Si was galvanostatically carried out at –155 mA cm^{-2} for 20 min. Figure 5 shows cross-sectional SEM images of the obtained specimen. A compact Si film is observed on a Ag substrate. This result confirms the feasibility of $SiCl_4$ gas as a Si source for Si deposition.

However, the smooth morphology is only observed in the vicinity of the substrate, and the deposits are granular in the outer layer. Such morphology is different from the deposit obtained at the similar concentrations of Si ions in KF–KCl–K_2SiF_6 molten salt (2.0–3.5 mol% K_2SiF_6) (12). The main factor giving the present morphological difference is likely the molar fraction of anion. Table 2 compares the anionic fraction of the melt after the addition of 2.00 mol% K_2SiF_6 and introduction of 2.30 mol% $SiCl_4$ into a eutectic KF–KCl melt. Here, it is assumed that Si(IV) ions exist in the form of SiF_6^{2-} due to the higher affinity of fluorine than chlorine as shown in Fig. 3, and that other ions exist as free ions. When 2.00 mol% of K_2SiF_6 is added to the melt, the anionic fraction of F^- ions is 44.1% which is almost the same order of Cl^- ions. On the other hand, exchange reaction between F^- ions and Cl^- ions occurs when $SiCl_4$ gas is supplied to the KF–KCl

molten salt. As the result, some free F^- ions form SiF_6^{2-} coordination and free Cl^- ions increase. After all, the anionic fraction of Cl^- ions (66.0 %) becomes as twice as that of F^- ions (31.6 %). Generally, compact and smooth Si layer has been electrodeposited in pure fluoride molten salts (18–20), the morphology in the present experiment seems to be influenced by the ratio of F^- and Cl^- ions, *i.e.*, the large amount of Cl^- ions is resposible for the granular deposit. The influence of the anionic molar ratio on the morphology of Si deposit is to be investigated in the future.

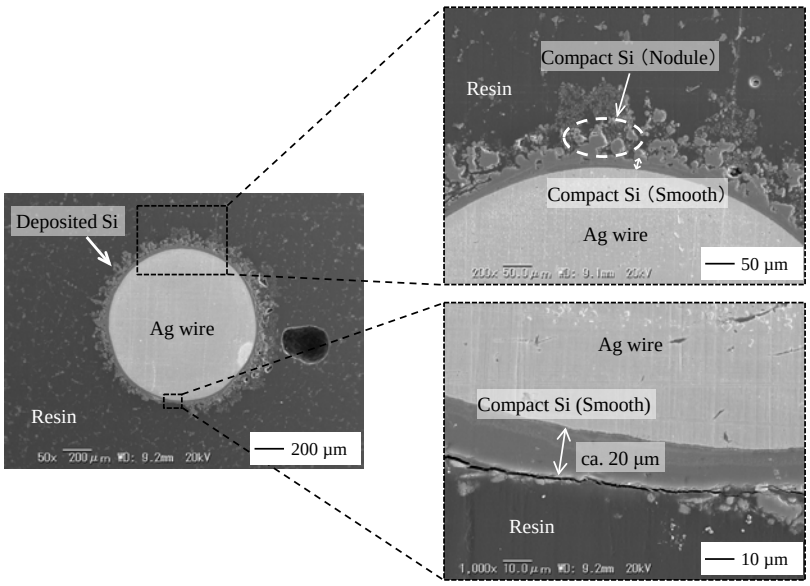

Figure 5 Cross-sectional SEM images of the sample obtained by the galvanostatic electrolysis of a Ag wire electrode at −155 mA cm^{-2} for 20 min in molten KF–KCl at 923 K after the introduction of $SiCl_4$.

Table 2 Anionic fraction of the melt after the addition of 2.00 mol% K_2SiF_6 and introduction of 2.30 mol% $SiCl_4$ into KF–KCl molten salt.

Si source	Anionic fraction / %		
	F^-	Cl^-	SiF_6^{2-}
K_2SiF_6 (2.00 mol%)	44.1	53.9	2.0
$SiCl_4$ (2.30 mol%)	31.6	66.0	2.4

Conclusions

The dissolution of $SiCl_4$ gas into KF–KCl molten salt and the electrodeposition of Si from the melt was investigated. By a gas transport method, a mixed Ar–$SiCl_4$ gas containing 14.90 g of $SiCl_4$ was bubbled into 200 g of a eutectic KF–KCl melt at 1023 K. The cyclic voltammetry suggested that a melt with 2.30 mol% of Si ion concentration was prepared. The dissolution efficiency of $SiCl_4$ was calculated to be 80% from the supplied amount (2.86 mol%) and the dissolved amount (2.30 mol%). The Si film was deposited on a Ag substrate at 923 K by galvanostatic electrolysis at –155 mA cm^{-2} for 20 min. By the cross-sectional SEM observation, a compact Si deposit was confirmed

though flatness was not good. The molar ratio of anions, F^-/Cl^-, is the possible cause to influence the morphology of the deposits.

Acknowledgments

This study was partly supported by the Core Research for Evolutionary Science and Technology (CREST) of the Japan Science and Technology Agency (JST).

References

1. U. Cohen and R. A. Huggins, *J. Electrochem.*, **123**, 381 (1976).
2. G. M. Rao, D. Elwell, and R. S. Feigelson, *J. Electrochem. Soc.*, **127**, 1940 (1980).
3. G. M. Rao, D. Elwell, and R. S. Feigelson, *J. Electrochem. Soc.*, **128**, 1708 (1981).
4. D. Elwell, *J. Crystal Growth*, **52**, 741 (1981).
5. D. Elwell and R. S. Feigelson, *Sol. Energ. Mat.*, **6**, 123 (1982).
6. D. Elwell, *J. Appl. Electrochem.*, **18**, 15 (1988).
7. L. P. Cook and H. F. McMurdie, *Phase Diagrams for Ceramists vol. VII*, The American Ceramic Society Inc., 509 (1989).
8. A. A. Andriiko, E. V. Panov, O. I. Boiko, B. V. Yakovlev, and O. Ya. Borovik, *Rus. J. Electrochem.*, **33**, 1343 (1997).
9. G. M. Haarberg, L. Famiyeh, A. M. Martinez, and K. S. Osen, *Electrochim. Acta*, **100**, 226 (2013).
10. K. Maeda, K. Yasuda, T. Nohira, R. Hagiwara, and T. Homma, *ECS Transactions, Molten Salts and Ionic Liquids*, **64**(4), 285 (2014).
11. K. Maeda, K. Yasuda, T. Nohira, R. Hagiwara, and T. Homma, *J. Electrochem. Soc.*, **162**, D444 (2015).
12. K. Yasuda, K. Maeda, T. Nohira, R. Hagiwara, and T. Homma, *J. Electrochem. Soc.*, **163**, D95 (2016).
13. R. Kubo, S. Nagakura, H. Iguchi and H. Ezawa, *Rikagaku Jiten, 4th Edition*, Iwanami Shoten, Tokyo (1987).
14. L. P. Cook and H. F. McMurdie, *Phase Diagrams for Ceramists vol. VII*, p. 509, The American Ceramic Society Inc., Columbus (1989).
15. M. W. Chase, Jr., *J. Phys. Chem. Ref. Data*, **9**, 1, (1998).
16. O. P. Prat, T. Cloitre and R. L. Aulombard, *Chem. Vap. Deposition*, **13**, 199 (2007).
17. T. Matsuda, S. Nakamura, K. Ide, K. Nyudo, S. Yae and Y. Nakato, *Chem. Lett.*, **7**, 569 (1996).
18. G. M. Rao, D. Elwell and R. S. Feigelson, *J. Electrochem. Soc.*, **127**, 1940 (1980).
19. D. Elwell and R. S. Feigelson, *Sol. Energy Mat.*, **6**, 123 (1982).
20. U. Cohen and R. A. Huggins, *J. Electrochem. Soc.*, **123**, 381 (1976).